NICST Internal Memo

Date: July 9, 2008
From: J McIntire, C. Pan, and S. Xiong
To: Bruce Guenther, Jim Butler, Jack Xiong
Subject: Radiometric Sensitivity of the VIIRS Sensor as Derived from the EDU RC-05 Part 1 Test (Nominal Plateau at 28V)

References:

[1] NICST_REPORT_08_024, "Updated Analysis Results for VIIRS EDU RC-05 Part 1, Nominal Plateau at 28V," J. McIntire, C. Pan, and S. Xiong, July 1, 2008.
[2] NICST_REPORT_06_009, 'Preliminary test analysis report of VIIRS EDU RC-05 Parts 1 & 2 in TV at Nominal Plateau,' August 4, 2006.
[3] NICST_REPORT_06_025, 'Radiometric Characterization Report of EDU RC-05 Part1 Using BCS at Hot Plateau (28V) and Comparison with Cold & Nominal,' December 13, 2006.
[4] Y21901, 'VIIRS Test Analysis report for RC-05, Part 1 Bands M12-M16, I4-I5,' Mina Mitani and Heidi Warner, January 17, 2007.
[5] 'Sensor Performance Verification Plan,' PVP154640-101.
[6] 'Performance Specification Sensor Specification,' ps154640-101c.

1. Introduction

The VIIRS EDU thermal vacuum test RC-05 Part 1 was designed to examine the sensor response to the Blackbody Calibration Source (BCS) in a near space-like environment. NICST analysis results for the nominal plateau portion of this test were reported for the radiometric gains and a number of associated specifications [1-3]. This work will focus on the sensitivity (SNR and NEdT) measurements, as an update to previous work [2-3] and as a comparison to other groups published work [4].

Table 1 lists the relevant UAIDs along with their corresponding BCS temperatures. Each collect contains 100 scans. The BCS source was located in the last collect window. In addition, the Space View Source (SVS) was positioned in the Space View (SV) port. The low gain region of band M13 was not considered. The VIIRS sensor was operated in diagnostic mode. The general outline of the methodology used in this work follows from [5] with some modifications.

2. Data Processing

The VIIRS EDU TV tests were conducted using the F9 aperture. However, all of the specifications for the VIIRS sensor assume a F6 aperture. In order to convert the requirement for comparison to the F9 data, the following factor was employed:

$$L_{F6} = L_{F9}\left(\frac{6}{9}\right)^2 . \quad (1)$$

Notice that it is the radiances that are scaled.

The data analyzed here is restricted to a subset of the available samples in a given collect for which the BCS source yielded a stable response. The following sample ranges were used in this work: samples 1650 – 1849 for M bands and samples 3300 – 3699 for I bands.

The response was analyzed using the sample method. First, the DN_{SV} was averaged over all samples in a given scan. Then, $<DN_{SV}>_{samples}$ was subtracted from each sample of the DN_{EV}. Next, the dn was averaged over scans, or $<dn>_{scans}$. The standard deviation of all scans for a specific sample was calculated, or σ_{scans}. Note that the HAM sides alternate from scan to scan such that there are 50 scans for each HAM side. Additionally, the I band data is divided into two subsamples where the larger for both SV and EV is always labeled subsample 1, to ensure the proper background subtraction.

The SNR is calculated by the usual method, as the ratio of the dn to the standard deviation. This calculation was preformed for each sample, or

$$SNR = \frac{1}{N}\sum_{i=0}^{N-1}\frac{\langle dn\rangle_{scans,i}}{\sigma_{scans,i}}, \quad (2)$$

where the sum is over all samples (N).

The temperatures (T_{xxx}) of the following were extracted: BCS, SVS, HAM, and Rotating Telescope Assembly (RTA). The HAM and RTA temperatures were acquired using the LRV extractor and the BCS and SVS temperatures were obtained from the gse files.

For each of these temperatures, a Planck radiation was calculated using the center wavelength (λ) of each band and the equation

$$L_{xxx}(\lambda, T_{xxx}) = \frac{2hc}{\lambda^5}\frac{1}{e^{hc/\lambda k T_{xxx}} - 1} . \quad (3)$$

Then, the in-band Relative Spectral Response (RSR) was applied as a correction to the Planck radiances; this was implemented by the following equation

$$\langle L_{xxx}(B,D,H,T_{xxx})\rangle = \frac{\int RSR(B,D,\lambda)\, L_{xxx}(B,H,T_{xxx})\, d\lambda}{\int RSR(B,D,\lambda)\, d\lambda}, \quad (4)$$

where B, D, and H represent band, detector, and HAM side, respectively. The RSR data was available for only some detectors; therefore, the existing RSR was extrapolated to the missing detectors.

Now we calculate the background subtracted source radiance, or

$$\Delta L_{BCS}\left(B,D,H,C\right) = rvs\left(B,\phi_{BCS},H\right)\left\langle L_{BCS}\left(B,D,C\right)\right\rangle - rvs\left(B,\phi_{SVS},H\right)\left\langle L_{SVS}\left(B,D,C\right)\right\rangle + \frac{rvs\left(B,\phi_{SVS},H\right) - rvs\left(B,\phi_{BCS},H\right)}{\rho_{RTA}\left(B\right)} \times \left\langle L_{RTA}\left(B,D,H,C\right)\right\rangle - \left(1-\rho_{RTA}\left(B\right)\right)\left\langle L_{HAM}\left(B,D,H,C\right)\right\rangle \quad . \quad (5)$$

This includes contributions to the background from not only the SVS, but from the RTA and HAM as well. In addition, the radiances are corrected for Response Versus Scan angle (RVS) and the reflectance factor (ρ) is included. Note that C refers to the collect number (each corresponding to a particular T_{xxx}) and that φ_{xxx} refers to the HAM angle of incidence for a given source (BCS or SVS).

Next, the SNR is modeled using the following function:

$$SNR = \frac{\Delta L_{BCS}}{\sqrt{b_0 + b_1 \Delta L_{BCS} + b_2 \Delta L_{BCS}^2}} . \quad (6)$$

The coefficients are determined by fitting this function to the data within the specified dynamic range. This equation is used to evaluate the SNR at L_{TYP}. For the bands M15, M16A, and M16B, the function must be extrapolated to L_{TYP}. In addition, Gaussian weighting ($1/\sigma^2$) was employed in the fitting, where

$$\sigma_{SNR_{sample}} = \sqrt{\frac{1}{N-1}\sum_{i=0}^{N-1}\left(SNR_{sample-i} - \left\langle SNR_{sample}\right\rangle\right)^2} . \quad (7)$$

The Noise Equivalent delta Temperature (NEdT) is computed via the equation

$$NEdT = \frac{\Delta L_{BCS}}{SNR \times \frac{\partial L}{\partial T}} . \quad (8)$$

The derivative is of the Planck radiance with respect to temperature evaluated at T_{TYP}. This NEdT is also determined at L_{TYP} using Equation (6), in order to compare with the specification SRV0053 (listed in Table 2).

3. Analysis

In Table 3, results of this analysis for the SNR and NEdT, both averaged over detectors, at T_{TYP} are presented. All of the detector averaged NEdT meet their respective requirements listed in Table 2. Here L_{TYP} is scaled to F9 using Equation (1). Only HAM side A is presented in this memo. The published Raytheon results are also included for comparison [5], except for bands M15, M16A, and M16B. For these bands, L_{TYP} lies outside of the range of measured values. As a result, the SNR and NEdT at L_{TYP} were determined by extrapolating Equation (6) beyond the measured range. Although the function in Equation (6) is nonlinear, this extrapolation is not that different from a straight line fit to the data at L_{TYP} for these bands. Raytheon did not compare to L_{TYP} for these three bands; instead they evaluated the SNR and NEdT at T=340 K (a temperature just inside the measured range). Consequently, the Raytheon results are considerably smaller for these bands.

The SNR and NEdT at L_{TYP} for each individual detector are listed in Tables 4 and 5. The detectors with NEdT that failed the specification are marked in red (detectors 1 and 10 in band M14). All other detectors meet the sensitivity requirement (SRV0053).

Figures 1 and 2 show the SNR plotted versus the background subtracted source radiance. This is graphed for each detector in each band along side its corresponding fitting residual. In Figure 3, the behavior of the SNR at L_{TYP} as a function of detector is shown. Again, detectors 1 and 10 in band M14 show low SNR curves that are Out Of Family (OOF).

The NEdT for all detectors graphed as a function of collect (or the corresponding BCS temperature listed in Table 1) in Figure 4. Figure 5 shows the NEdT at L_{TYP} for each detector. Band M14, detectors 1 and 10 fail the specification (dashed red lines in Figure 5). All other bands and detectors meet the requirement.

Detectors 1 and 10 for band M14 show large standard deviations for each individual sample as a function of scans (about 2 and 4 times the standard deviations of other detectors in M14, respectively). This indicates a larger variation with respect to time. The standard deviations are smaller (about 1 and 2 times the values of other detectors in M14, respectively) for each individual scan as a function of sample, which indicative of larger spatial variation for detector 10. In addition, the $<dn>_{scans}$ for detector 1 is roughly 50 % of the other detectors in band M14. As a result of the spatial and temporal variations (as well as the small $<dn>_{scans}$ for detector 1), the SNR is low and OOF and the NEdT is high and OOF for both detectors. Thus, we conclude that detectors 1 and 10 for band M14 are noisy.

4. Summary

- NEdT at L_{TYP} meet the requirement for all bands and detectors, with the exception of detectors 1 and 10 in band M14.
- SNR at L_{TYP} are in good agreement with the published findings of Raytheon [4], except bands M15, M16A, and M16B. Different temperatures were used for NICST (T_{TYP}) and Raytheon (T=340).
- Detectors 1 and 10 for band M14 are noisy.

Acknowledgement

The sensor test data used in this document was provided by the SBRS testing team. Approaches for data acquisition and data reductions, as well as data extraction tools were also provided by the SBRS. We would like to thank the SBRS team for their support. The data analysis tools were developed by the NICST team, and we would like to extend our gratitude for their valued assistance.

Table 1: EDU RC-05 Part 1 UAIDs with corresponding BCS temperatures.

UAID	BCS Temperature (K)
2002504	190.1
2002505	209.9
2002506	229.6
2002507	240.1
2002508	247.2
2002509	255.2
2002510	262.0
2002511	270.4
2002512	278.0
2002513	285.3
2002514	291.9
2002515	299.9
2002516	306.8
2002517	314.9
2002518	320.7
2002519	326.8
2002520	331.8
2002521	335.9
2002522	340.0
2002523	345.0

Table 2: NEdT at L_{TYP} specification (SRV0053) [6].

Band	T_{TYP}	NEdT at T_{TYP}
I4	270	2.500
I5	210	1.500
M12	270	0.396
M13 hg	300	0.107
M14	270	0.091
M15	300	0.070
M16A	300	0.072
M16B	300	0.072

Table 3: Detector averaged SNR and NEdT at L_{TYP} (HAM side A).

Band	Raytheon [4]	SNR at L_{TYP}	NEdT at L_{TYP}
I4	49.9	48.1	0.41
I5	71.4	78.2	0.457
M12	191	198	0.101
M13 hg	678	661	0.039
M14	813	950	0.052
M15	2058	3107	0.022
M16A	1646	2237	0.033
M16B	1601	2214	0.034

Table 4: SNR at L_{TYP} for each band and detector (HAM side A).

Detector	I4	I5	M12	M13 hg	M14	M15	M16A	M16B
1	46.5	88.5	209	667	445	3185	2338	2254
2	45.7	79.8	207	652	1056	2563	2174	1986
3	46.7	82.0	218	708	1031	3101	2264	2740
4	46.6	80.3	210	576	1011	3440	2090	2009
5	43.9	75.3	219	682	910	3819	2278	2218
6	43.6	58.7	211	637	1162	2839	2169	2087
7	48.6	80.8	215	671	1034	2571	2855	2612
8	48.0	67.4	206	656	1020	3601	2238	2233
9	50.1	79.6	215	668	972	3099	2086	2158
10	49.5	86.4	211	672	306	3432	1980	2210
11	49.3	76.6	198	660	1019	2693	2418	2349
12	48.8	85.0	142	690	1244	4470	2099	2131
13	49.0	79.0	182	672	1157	3125	2132	2139
14	49.3	80.0	200	654	1014	2649	2020	1946
15	49.5	63.7	155	658	943	2919	2184	2095
16	48.8	87.7	163	658	875	2210	2469	2249
17	49.8	87.0	~	~	~	~	~	~
18	50.5	75.9	~	~	~	~	~	~
19	49.7	81.9	~	~	~	~	~	~
20	49.4	83.0	~	~	~	~	~	~
21	49.9	81.2	~	~	~	~	~	~
22	48.0	73.0	~	~	~	~	~	~
23	48.4	81.6	~	~	~	~	~	~
24	48.3	71.3	~	~	~	~	~	~
25	48.6	81.3	~	~	~	~	~	~
26	47.1	78.3	~	~	~	~	~	~
27	49.1	75.3	~	~	~	~	~	~
28	47.5	79.8	~	~	~	~	~	~
29	48.8	69.2	~	~	~	~	~	~
30	47.4	77.4	~	~	~	~	~	~
31	46.8	79.5	~	~	~	~	~	~
32	47.4	77.0	~	~	~	~	~	~

Table 5: NEdT at L_{TYP} for each band and detector (HAM side A).

Detector	I4	I5	M12	M13 hg	M14	M15	M16A	M16B
1	0.42	0.40	0.094	0.038	0.097	0.021	0.032	0.033
2	0.43	0.44	0.095	0.039	0.041	0.026	0.034	0.037
3	0.42	0.44	0.090	0.036	0.042	0.021	0.033	0.027
4	0.42	0.45	0.093	0.044	0.043	0.019	0.035	0.037
5	0.45	0.48	0.090	0.037	0.048	0.017	0.032	0.033
6	0.45	0.60	0.093	0.040	0.037	0.023	0.034	0.035
7	0.41	0.44	0.091	0.038	0.042	0.026	0.026	0.028
8	0.41	0.52	0.095	0.039	0.042	0.019	0.033	0.033
9	0.39	0.44	0.091	0.038	0.045	0.022	0.035	0.034
10	0.40	0.41	0.093	0.038	0.14	0.019	0.037	0.033
11	0.40	0.46	0.099	0.039	0.042	0.025	0.031	0.031
12	0.40	0.42	0.138	0.037	0.035	0.015	0.035	0.035
13	0.40	0.45	0.108	0.038	0.037	0.021	0.035	0.035
14	0.40	0.45	0.098	0.039	0.043	0.025	0.037	0.038
15	0.40	0.55	0.127	0.039	0.046	0.023	0.034	0.035
16	0.40	0.40	0.121	0.039	0.050	0.030	0.030	0.033
17	0.40	0.41	~	~	~	~	~	~
18	0.39	0.47	~	~	~	~	~	~
19	0.40	0.44	~	~	~	~	~	~
20	0.40	0.43	~	~	~	~	~	~
21	0.40	0.44	~	~	~	~	~	~
22	0.41	0.49	~	~	~	~	~	~
23	0.41	0.43	~	~	~	~	~	~
24	0.41	0.49	~	~	~	~	~	~
25	0.41	0.44	~	~	~	~	~	~
26	0.42	0.45	~	~	~	~	~	~
27	0.40	0.47	~	~	~	~	~	~
28	0.42	0.44	~	~	~	~	~	~
29	0.40	0.51	~	~	~	~	~	~
30	0.42	0.46	~	~	~	~	~	~
31	0.42	0.45	~	~	~	~	~	~
32	0.42	0.46	~	~	~	~	~	~

Figure 1: SNR versus background subtracted source radiance for bands I4, I5, M12, and M13 hg with fitting residuals.

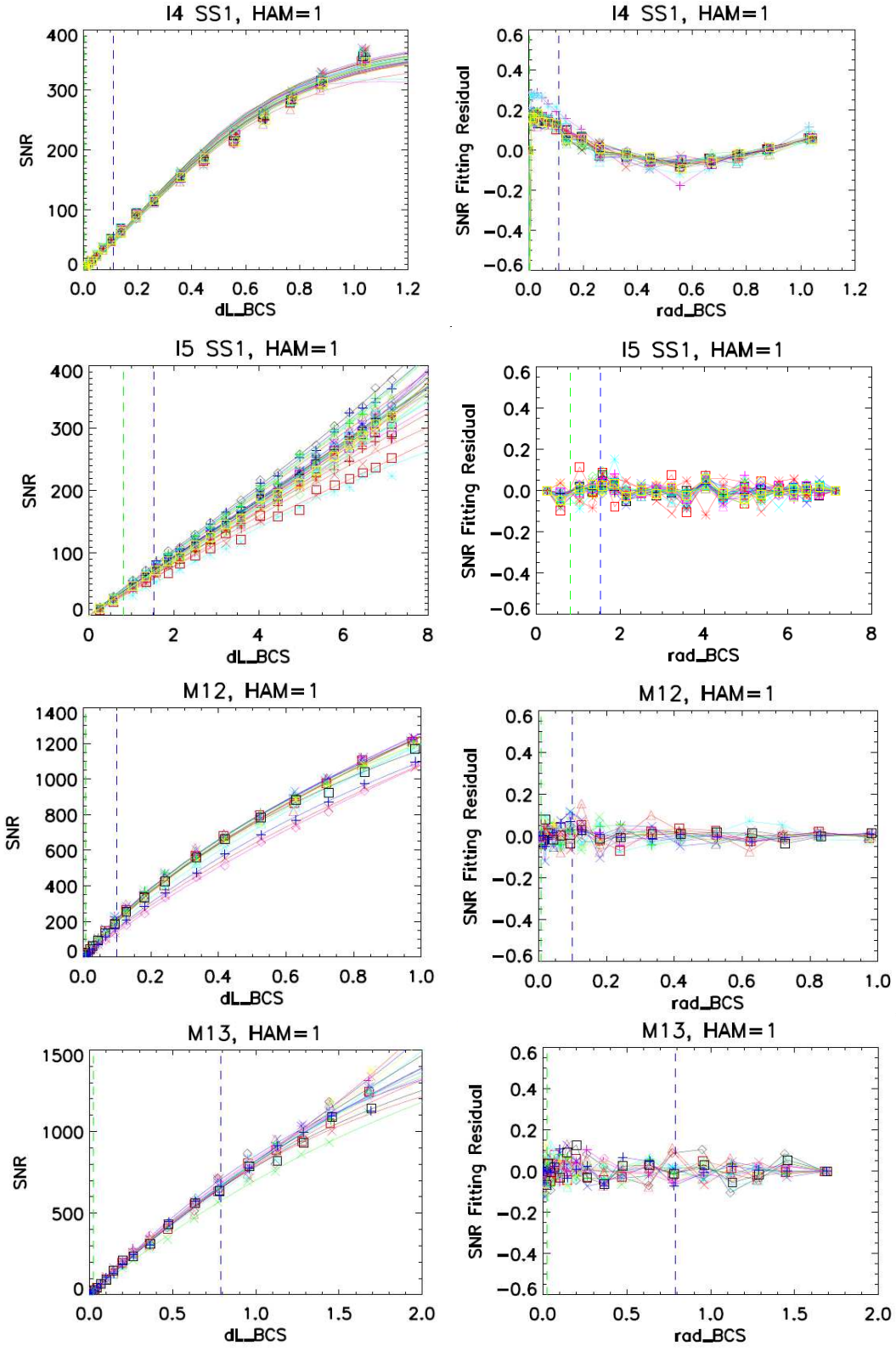

Figure 2: SNR versus background subtracted source radiance for bands M14, M15, M16A, and M16B with fitting residuals.

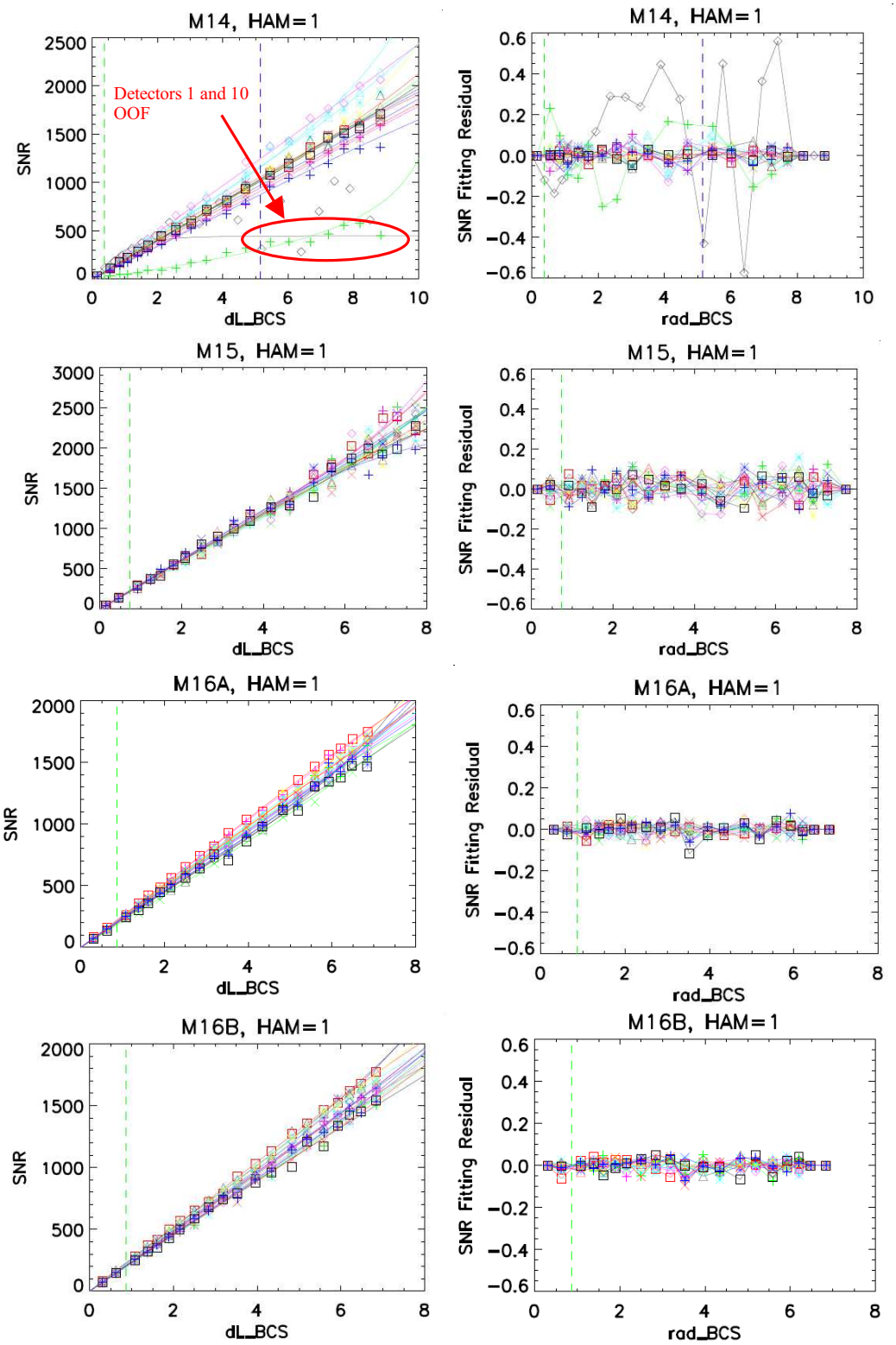

Figure 4: SNR at L_{TYP} for all bands as a function of detector.

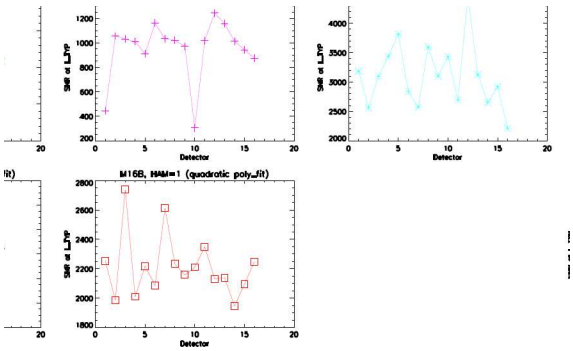

Figure 4: NEdT versus dL_BCS for all bands and detectors.

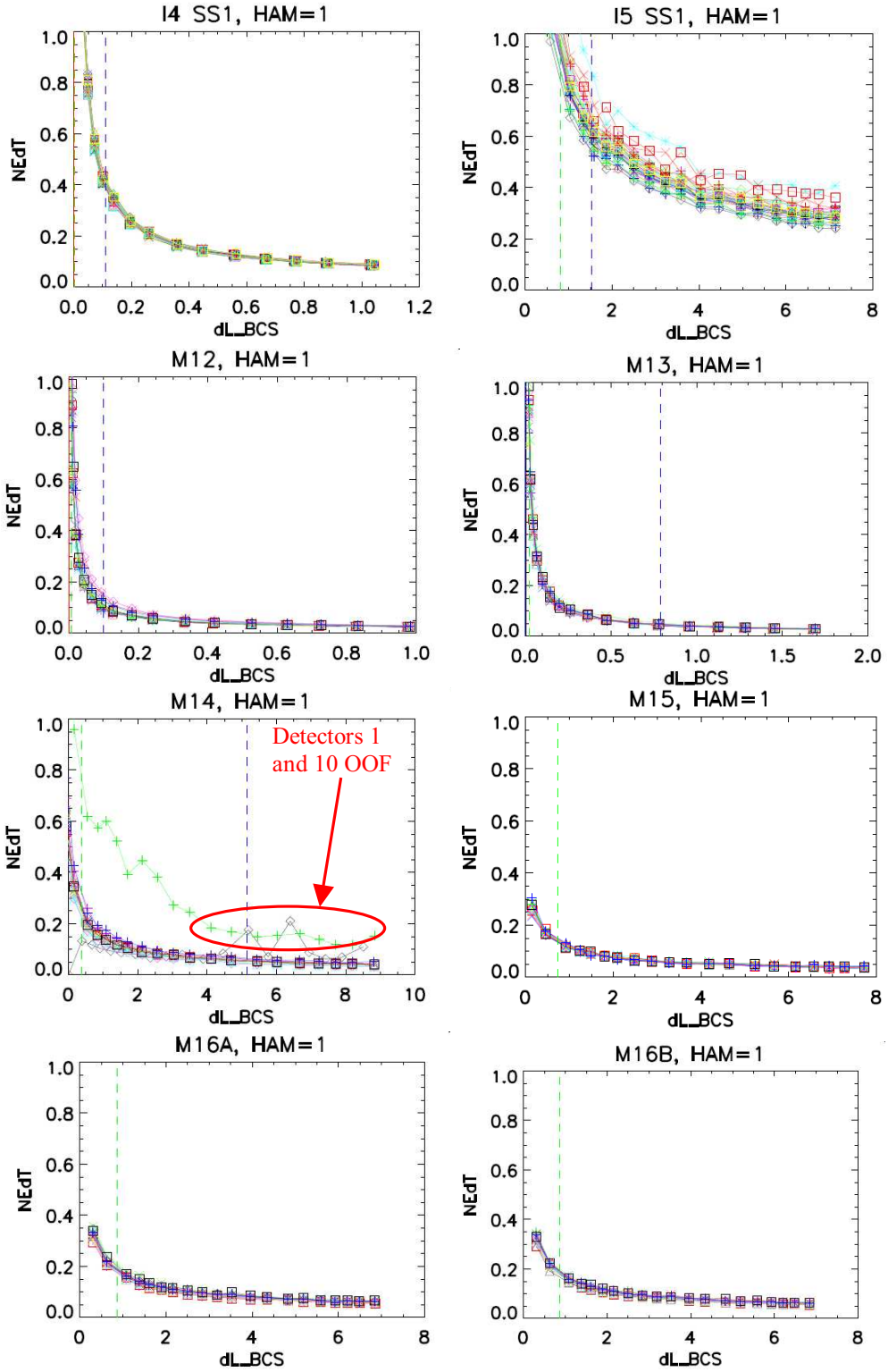
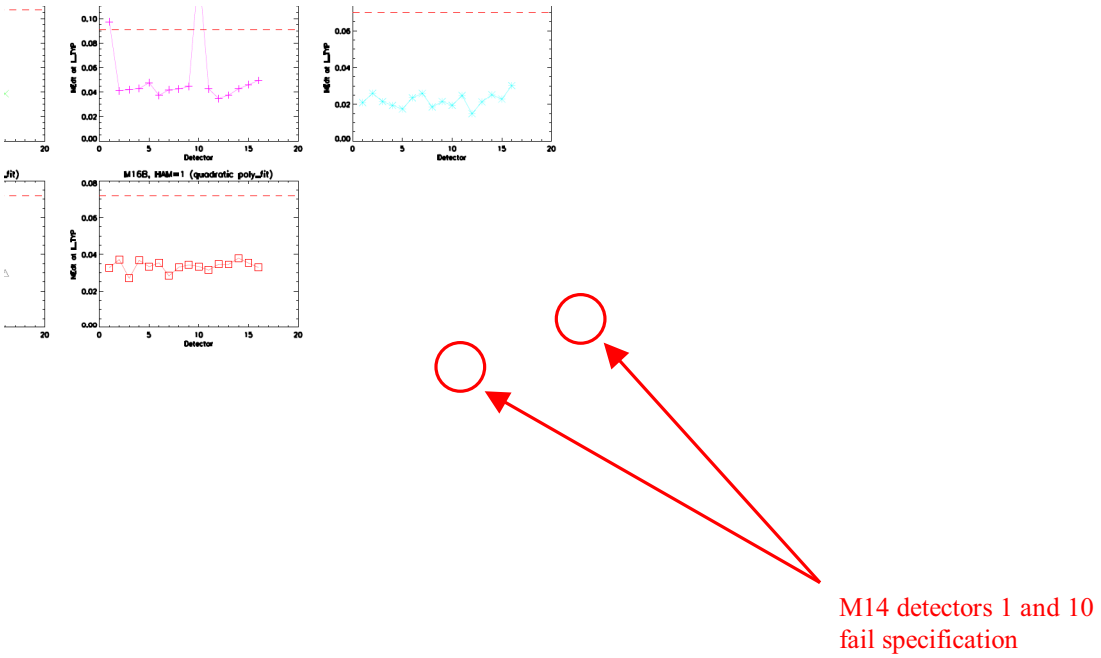
Figure 5: NEdT at L_{TYP} for all bands as a function of detector.